

## Parallel generation of nanochannels in fused silica with a single femtosecond laser pulse: Exploiting the optical near fields of triangular nanoparticles

F. Hubenthal,<sup>a)</sup> R. Morarescu, L. Englert, L. Haag, T. Baumert, and F. Träger  
*Institut für Physik and Center for Interdisciplinary Nanostructure Science and Technology (CINSaT),  
 Universität Kassel, Heinrich-Plett-Str. 40, 34132 Kassel, Germany*

(Received 7 May 2009; accepted 6 July 2009; published online 10 August 2009)

We present experiments to prepare highly ordered nanochannels with subdiffraction dimensions on fused silica surfaces with femtosecond laser light. For this purpose, we exploit the strongly enhanced near field of highly ordered triangular gold nanoparticles. We demonstrate that after a single laser shot, 6  $\mu\text{m}$  long nanochannels with a mean depth of 4 nm and an average width of 96 nm, i.e., well below the diffraction limit, are generated. These nanochannels are prepared by ablation, caused by the localization of the near field. The crucial parameters, besides the applied fluence, are the polarization direction of the incoming laser light with respect to the triangular nanoparticles and the size of the nanoparticles. © 2009 American Institute of Physics.

[DOI: 10.1063/1.3186787]

For nearly all aspects in modern nanotechnology, there is an ongoing interest in further miniaturization of surface structures with sizes well below the diffraction limit. One prominent example is the investigation of confinement on the static and dynamic properties of DNA, necessary for the design of devices for single molecule analysis and manipulation.<sup>1</sup> A versatile possibility to obtain such nano-scale structures is to focus light by nanoantennas,<sup>2,3</sup> which typically are noble metal nanoparticles (NPs) that exhibit well developed localized surface plasmon polariton resonances (SPRs). Due to the excitation of SPRs as well as due to a focusing effect of the NPs,<sup>4</sup> localized and extremely high optical near fields in very tiny areas can be generated. Note that also direct laser writing of subdiffraction structures in dielectrics was recently reported either via tailoring the energy flux on the femtosecond time scale or by making use of point spread function engineering.<sup>5-7</sup>

In recent publications light induced large area patterning of surfaces with structures well below the diffraction limit has been achieved using spherical  $\text{SiO}_2$  or latex beads as well as triangular NPs.<sup>8-12</sup> Depending on the direction and polarization of the incoming laser light, different nanopatterns have been created. So far, only small round or elongated holes with subdiffraction dimensions have been generated. In this letter, we demonstrate that nanochannels with a depth of a few nanometers, a width of several tens of nanometers, and a length of several micrometers can be prepared with high accuracy using highly ordered triangular gold NP arrays. This opens another dimension in nanostructuring of surfaces for advanced applications in modern nanotechnology.

First, regular arrays of triangular gold NPs were prepared utilizing nanosphere lithography.<sup>13</sup> Quadratic fused silica plates with a length of 12 mm served as substrates and latex spheres with a diameter of  $D=330$  nm were used as a lithographic mask. In brief, a monolayer of the spheres has been arranged in a hexagonal order on a substrate by drop

coating. After the formation of the nanosphere mask, a gold film with a thickness of 30 nm was deposited on the substrate by thermal evaporation. Afterward, the nanosphere mask was removed by sonicating the substrate for 3 min in dichloromethane. Within the 3 min sonication time all nanospheres have been removed, leaving behind large areas with highly ordered triangular gold NPs. In these NP arrays, marks have been written with laser light, which allow to determine the polarization direction of the laser light with respect to the orientation of the triangular NPs on the substrate.

Subsequently, the samples with the triangular NPs were irradiated with a single femtosecond light pulse, delivered by an amplified Ti:sapphire laser system, coupled to a modified microscope setup. Figure 1 depicts a schematic of the experimental setup for the irradiation experiments. The pulse duration in the interaction region was 35 fs full width at half maximum. Details of the experimental setup of the laser system have been described elsewhere.<sup>7</sup> The NP arrays were irradiated under ambient conditions using linearly polarized light under normal incidence with a central wavelength of  $\lambda=790$  nm. The diameter of the laser spot on the sample was set to 32  $\mu\text{m}$ . The effect of different pulse energies on the generated nanostructures has been studied, exploiting the Gaussian intensity profile of the laser light. Measurements at different distances from the center of the laser spot yield the generated nanostructures as a function of applied energy. By

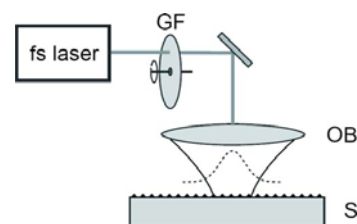


FIG. 1. (Color online) Schematic of experimental setup. The energy of the femtosecond laser pulse is controlled by a neutral density gradient filter (GF) and focused by a microscope objective (OB) on the substrate (S) containing the NPs. The substrate surface is shifted relative to the focal plane of the objective leading to an increased spot diameter of 32  $\mu\text{m}$ . The Gaussian intensity profile at the substrate surface is sketched (dashed line).

<sup>a)</sup> Author to whom correspondence should be addressed. Electronic mail: hubentha@physik.uni-kassel.de.

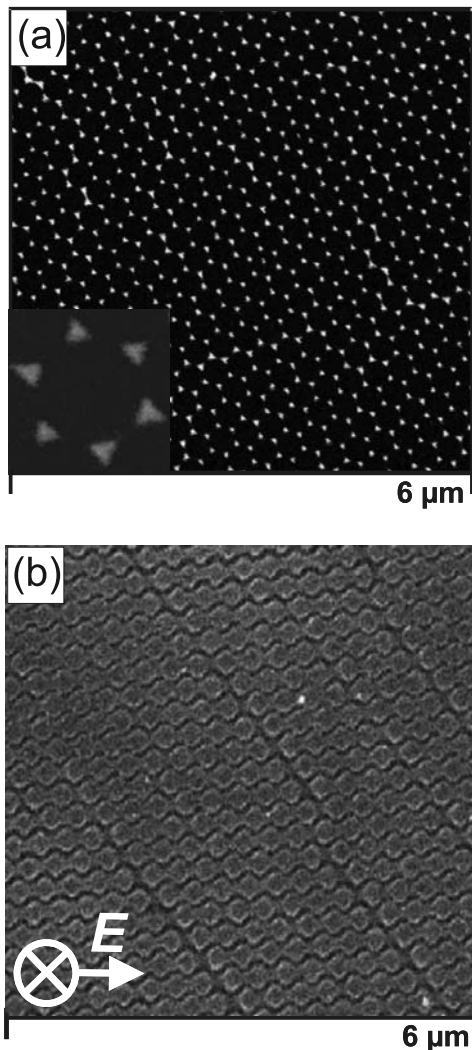


FIG. 2. (a) Highly ordered triangular NPs prepared by nanosphere lithography. (b) Nanochannels generated by ablation and mediated by the near field. The arrow indicates the polarization direction of the laser light.

this means a complete set of nanostructures on the substrates was obtained after a single shot experiment. In order to increase the energy range, the applied pulse energy has been varied between  $E=0.1 \mu\text{J}$  and  $E=7.0 \mu\text{J}$ . After irradiation, the samples were cleaned in aqua regia for 2 h and subsequently sonicated in distilled water to remove residual material.

The NPs as well as the generated nanochannels have been characterized by atomic force microscopy (AFM), scanning electron microscopy (SEM), and extinction spectroscopy. Figure 2(a) depicts a SEM image of the highly ordered triangular gold NPs on a fused silica substrate. The inset of Fig. 2(a) is a magnification, showing the triangular shape of the NPs, which exhibit a side length of  $(74 \pm 6)$  nm and an average tip to tip distance of  $(102 \pm 14)$  nm. We emphasize that no damages of the gold NPs due to the sonicating have been observed. The average height of the NPs has been determined by means of AFM to be  $(30 \pm 4)$  nm. Since a thermal deposition process has been used, a small variation in the NP height occurs. The extinction spectrum (not shown) of the triangular gold NPs is dominated by a strong SPR at  $\lambda=730$  nm due to the excitation of the dipolar SPR-mode.<sup>14</sup>

As mentioned before, the NPs were irradiated under ambient conditions with a single femtosecond light pulse. The wavelength of  $\lambda=790$  nm is close to the dipolar SPR and

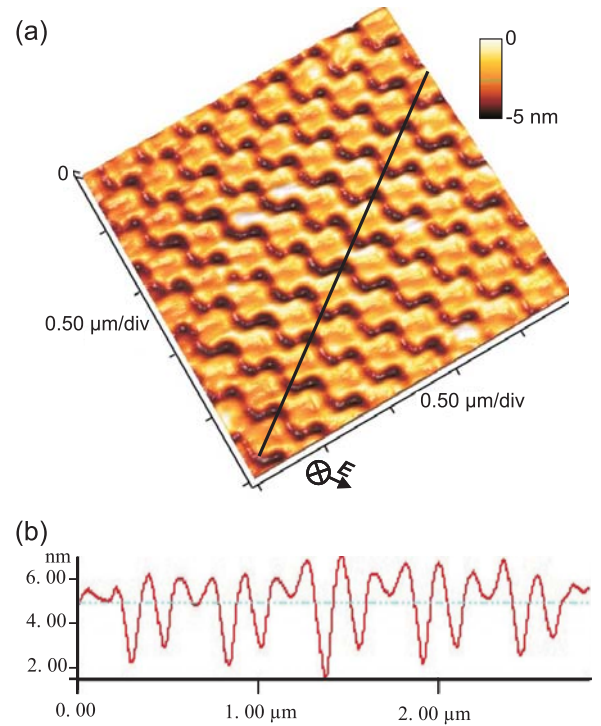


FIG. 3. (Color online) (a) Large scale AFM image of the generated nanochannels, which are oriented along the polarization of the laser light (arrow). From such large scale AFM images, height profiles have been taken to determine the channel length and width. (b) Height profile along the black line in (a). The evaluation of a set of height profiles reveals an average depth of the channels of  $\langle D \rangle = (4.0 \pm 0.6)$  nm and an average width of  $\langle W \rangle = (96 \pm 4)$  nm, which has been measured at the substrate surface level.

able to create high field enhancements at the tips of the NPs.<sup>12</sup> A detailed AFM analysis revealed that for similar applied pulse energies, similar nanostructures in the substrate surface have been created. It turned out that for low energies, only small holes are generated, while for increasing energies these holes become elongated, merge together, and finally form nanochannels at high energies. However, if the energy of the laser light exceeds the ablation threshold energy of the substrate [ $\approx 2 \text{ J/cm}^2$  (Refs. 7 and 15)], direct ablation of the substrate material at the central part of the laser spot is observed. A detailed description of all generated nanostructures will be given elsewhere.<sup>16</sup> In this letter, we present the most intriguing generated structures: nanochannels. The presented nanochannels have been obtained in a circular ring area with an inner diameter of  $3 \mu\text{m}$  and an outer diameter of  $9 \mu\text{m}$  around the center of the laser spot, after irradiation with a pulse energy of  $E=3.8 \mu\text{J}$ . Note that due to the laser spot diameter of  $32 \mu\text{m}$ , the average fluence was only  $F \approx 0.5 \text{ J/cm}^2$ , i.e., below the ablation threshold of fused silica.

Figure 2(b) displays a SEM image of a sample after irradiation with a single femtosecond pulse and subsequent cleaning. The image shows clearly that nanochannels with a length of at least  $6 \mu\text{m}$  have been generated. We emphasize that in the presented results, the length was limited by the experimental conditions due to the Gaussian intensity profile of the laser light. The width and the depth of the nanochannels in the fused silica substrate were measured by means of AFM. Figure 3(a) shows such an AFM image demonstrating that highly ordered nanochannels have been generated. The corresponding height profile is displayed in Fig. 3(b). From a set of height profiles, we obtained an average lateral width of

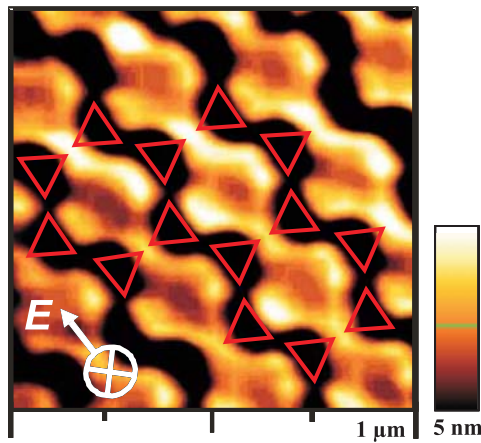


FIG. 4. (Color online) A magnified AFM image of the generated nanochannels. The triangles indicate the original position of the triangular NPs on the substrate. The white arrow shows the polarization direction of the incoming laser light.

the nanochannels of  $\langle W \rangle = (96 \pm 4)$  nm and an average depth of  $\langle D \rangle = (4.0 \pm 0.6)$  nm. Hence, nanochannels with dimensions well below the diffraction limit have been generated.

To explain the generated nanochannels one has to consider the polarization direction of the incoming laser light with respect to the orientation of the triangular NPs. Figure 4 depicts an AFM image of the nanochannels with a higher resolution. In addition, the initial position of the triangular NPs and the polarization direction of the laser light are marked.

It has been shown<sup>12,17</sup> that for the present configuration, i.e., for well separated triangular NPs with a side length smaller than 200 nm and a polarization along a base of the triangles, the highest field concentration is located only at the two tips of the basis parallel to the polarization. Due to their hexagonal arrangement, the local fields of neighboring excited NP tips overlap. This leads to a homogeneous ablation of material along the excited base of the triangular NPs and thus to the formation of the nanochannels.

The most crucial parameter for the presented experiments is the orientation of the polarization of the laser light with respect to the triangular NPs. Only if the polarization is parallel to a base of a triangle, a field enhancement with the same strength at the two tips of this basis is generated.<sup>12,17</sup> As we will demonstrate in a following publication,<sup>16</sup> for a polarization perpendicular to a base of the triangles, nanogrooves with a bonelike shape are generated. Another crucial parameter is the size of the NPs. They must be small enough to permit a sufficient overlap of the enhanced fields of neighboring tips such that a homogeneous ablation of material can take place, which is necessary to create uniform nanochannels. Only triangular NPs with a side length significant below 200 nm that are closely packed in hexagonal order permit large enough overlap of the local fields to generate micrometer long nanochannels. For larger NPs discontinuous

structures result as a consequence of the localization of the local fields.<sup>11</sup> As mentioned previously, the height of NPs and, hence, the spectral positions of their SPRs vary a little. However, this has only minor effects on our experiments since the wavelength of the laser light is not exactly in resonance with the SPR of the NPs. As it will be shown in Ref. 16, the fluence determines the width and the depth of the nanochannels. The length depends only on the area in which highly ordered triangular NPs are arranged and on the area, which is homogeneously illuminated by the laser light.

In summary, we have demonstrated that micrometer long nanochannels with a depth of only several nanometer and a width of less than 100 nm, i.e., well below the diffraction limit, can be created in fused silica surfaces. While the width and the depth of the nanochannels are determined by the applied fluence, the length of the channels is mainly limited by the quality of the prepared NP arrays. To obtain these structures, the near field of triangular NPs, which have been irradiated with a single femtosecond light pulse, has been exploited. The results presented in this letter open another dimension for applications in modern nanotechnology.

Financial support from the German Science Foundation and the European Commission under Contract No. MRTN-CT-2003-504233 is gratefully acknowledged.

- <sup>1</sup>D. J. Bonhuis, C. Meyer, D. Stein, and C. Dekker, *Phys. Rev. Lett.* **101**, 108303 (2008).
- <sup>2</sup>S. Kühn, U. Håkanson, L. Rogobete, and V. Sandoghdar, *Phys. Rev. Lett.* **97**, 017402 (2006).
- <sup>3</sup>R. M. Bakker, H.-K. Yuan, Z. Liu, V. P. Drachev, A. V. Kildishev, V. M. Shalaev, R. H. Pedersen, S. Gresillon, and A. Boltasseva, *Appl. Phys. Lett.* **92**, 043101 (2008).
- <sup>4</sup>N. N. Nedyalkov, H. Takada, and M. Obara, *Appl. Phys. A* **85**, 163 (2006).
- <sup>5</sup>M. Merano, G. Boyer, A. Trisorio, G. Chériaux, and G. Mourou, *Opt. Lett.* **32**, 2239 (2007).
- <sup>6</sup>L. Englert, M. Wollenhaupt, L. Haag, C. Sarpe-Tudoran, B. Rethfeld, and T. Baumert, *Appl. Phys. A: Mater. Sci. Process.* **92**, 749 (2008).
- <sup>7</sup>L. Englert, B. Rethfeld, L. Haag, M. Wollenhaupt, C. Sarpe-Tudoran, and T. Baumert, *Opt. Express* **15**, 17855 (2007).
- <sup>8</sup>R. Denk, K. Piglmayer, and D. Bäuerle, *Appl. Phys. A: Mater. Sci. Process.* **74**, 825 (2002).
- <sup>9</sup>N. Nedyalkov, T. Sakai, T. Miyayoshi, and M. Obara, *Appl. Phys. Lett.* **90**, 123106 (2007).
- <sup>10</sup>W. Guo, Z. B. Wang, L. Li, D. J. Whitehead, B. S. Luk'yanchuk, and Z. Liu, *Appl. Phys. Lett.* **90**, 243101 (2007).
- <sup>11</sup>P. Leiderer, C. Bartels, J. König-Birk, M. Mosbacher, and J. Boneberg, *Appl. Phys. Lett.* **85**, 5370 (2004).
- <sup>12</sup>J. Boneberg, J. König-Birk, H.-J. Münzer, P. Leiderer, K. L. Shuford, and G. C. Schatz, *Appl. Phys. A: Mater. Sci. Process.* **89**, 299 (2007).
- <sup>13</sup>U. C. Fischer and H. P. Zingsheim, *J. Vac. Sci. Technol.* **19**, 881 (1981).
- <sup>14</sup>K. L. Shuford, M. A. Ratner, and G. C. Schatz, *J. Chem. Phys.* **123**, 114713 (2005).
- <sup>15</sup>M. Lenzner, J. Krüger, S. Sartania, Z. Cheng, C. Spielmann, G. Mourou, W. Kautek, and F. Krausz, *Phys. Rev. Lett.* **80**, 4076 (1998).
- <sup>16</sup>R. Morarescu, L. Englert, L. Haag, T. Baumert, F. Träger, and F. Hubenthal (unpublished).
- <sup>17</sup>E. Hao and G. C. Schatz, *J. Chem. Phys.* **120**, 357 (2004).